Annual Progress Report for JFY 2006

March 5, 2007

# CDF Experiment

Spokespersons
Japan S. Kim (University of Tsukuba)
U.S.A. R. Roser (Fermilab) and J. Konigsberg (University of Florida)

The year 2006 marked the sixth year for the Tevatron Run-II program and the CDF Run-II experiment.The improvement in the accelerator performance seen in years from 2003 to 2005 continued in 2006. The instantaneous luminosity at the beginning of the stores consistently exceeds the design luminosity of $\mathcal{L} = 2\times10^{32}$ cm$^{-2}$ s$^{-1}$, and the record luminosity is $2.9 \times 10^{32}$ cm$^{-2}$ s$^{-1}$ as of the end of February 2007 (Figure 1 (top)). A weekly integrated luminosity in excess of 40 pb$^{-1}$ has also been achieved. The total integrated luminosity in the calendar year 2006 amounts to about 800 pb$^{-1}$ despite a long shutdown in spring, and the Run II total to date has exceeded 2.5 fb$^{-1}$ (Figure 1 (bottom)).

The upgraded CDF detector has been functioning very well with high efficiency. The integrated luminosity recorded by CDF amounts to roughly 2.0 fb$^{-1}$, roughly 20 times that of Run I (Figure 2). We expect to collect a total of 4 to 8 fb$^{-1}$ before the Tevatron shuts down. For operations at a high luminosity, the CDF detector have completed upgrades to some of the detector components, in particular the DAQ system that allows efficient data taking and data logging. They include the upgrades to the silicon-based trigger system (SVT) and to the consumer server/logger system (CS/L).

CDF has analyzed about 1 fb$^{-1}$ of data thus far, and many important and interesting results have emerged from Run-II data. We summarize these physics results, as well as detector upgrade efforts, with an emphasis on contributions from the Japan group.

## 1 Physics Results

### 1.1 Electroweak physics

A measurement of the $W^{\pm}$ boson mass using the Run-II data has become available for the first time. Figure 3 shows the transverse mass distribution of the lepton (electron or muon) and missing transverse energy system for $W^\pm \to \ell^\pm \nu$ candidates from a data set corresponding to first 200 $\mathrm{pb}^{-1}$ of Run-II data. These events have lead to the first measurement of the $W^\pm$ boson mass in Run II [1] :

$$m_W = 80413 \pm 48\ \mathrm{MeV}/c^2,$$

where the total uncertainty of 48 $\mathrm{MeV}/c^2$ represents the single most precise measurement of the quantity, as illustrated in Figure 4. The impact of this measurement on constraints on the Higgs boson mass will be discussed later in this document. With 1.5 $\mathrm{fb}^{-1}$ of data that CDF has collected already, the $W^\pm$ boson mass will be measured with a precision of about 25 $\mathrm{MeV}/c^2$. Combined with top quark mass measurements, it will provide constraints on the Higgs boson mass with a relative precision of 20%.

Another area of study concerns pair production of gauge bosons. The unified electroweak theory has a non-Abelian gauge structure, resulting in self-couplings of the gauge bosons, such as $W^+W^-Z^0$ and $W^+W^-\gamma$ vertices.

Associated production of a $W^\pm$ boson and a $Z^0$ boson has been observed for the first time. The leptonic decays of the $W^\pm$ and $Z^0$ bosons are used, leading to a very distinctive signature of three energetic leptons, a large transverse missing energy, and no extra jets. The production cross section is measured to be $\sigma(\bar{p}p \to W^\pm Z^0 X) = 5.0\,^{+1.8}_{-1.6}$ pb, consistent with a theory prediction of $3.7 \pm 0.3$ pb.

Production of $W^\pm\gamma$ pairs is also studied. 855 candidate events with photons above 7 $\mathrm{GeV}/c$ have been observed in the $W \to \mu\nu$ channel among 1 $\mathrm{fb}^{-1}$ of data. Kinematic distributions such as photon transverse momentum distribution and the transverse mass of the lepton-photon-missing $E_T$ system are examined (Figure 5). A good agreement with expectations is found. The production cross section is measured to be $\sigma(\bar{p}p \to W\gamma X) \cdot \mathcal{B}(W \to \ell\nu) = 19.11 \pm 1.04 \pm 2.40 \pm 1.11$ pb [2], in very good agreement with theory prediction of $19.3 \pm 0.4$ pb. A. Nagano (Tsukuba) has performed the analysis.

## 1.2 Top quark properties

Since its discovery by CDF in 1995, the top quark and its properties have been studied extensively. With increased statistics of Run-II data, these studies are now performed with precision.

The top quark analyses with Run-II data include measurements of the mass and production cross section using various decay channels. The production cross section has been measured in di-lepton, lepton + jet and all-hadronic channels. In the lepton + jet channel with secondary vertex $b$-jet tagging, the $t\bar{t}$ production cross section is measured to be $\sigma = 8.2 \pm 0.6 \pm 1.0$ pb [3]. The corresponding cross section from the di-lepton channel is $\sigma = 8.3 \pm 1.5 \pm 1.1$ pb [4]. The all-hadronic channel measures $\sigma = 8.3 \pm 1.0\,^{+2.0}_{-1.5} \pm 0.5$ pb [5]. They all are in agreement with a next-to-leading order QCD calculation of $6.7\,^{+0.71}_{-0.88}$ pb for $m_{\mathrm{top}} = 175\ \mathrm{GeV}/c^2$. Y. Kusakabe, J. Naganoma (Waseda), and T. Kubo, T. Masubuchi

(Tsukuba) have contributed to the lepton + jet channel analysis, and N. Kimura and Y. Takeuchi (Tsukuba) to the di-lepton analysis.

The top quark mass is extracted using various techniques, both from the lepton + jet channel and the dilepton channel. K. Sato, T. Tomura and T. Maruyama (Tsukuba) have used the lepton + jet channel and applied the looser second $b$-jet tagging method called "jet probability tags" in addition to the tighter "SECVTX" tags. Tagging two $b$-quark jets is particularly important in mass measurements, because it reduces not only the background but also the number of combinations that have to be considered in a given $t\bar{t}$ event. The reconstructed mass distribution is shown in Figure 6, and the extracted mass value is $m_{\mathrm{top}} = 173.4 \pm 2.5 \pm 1.3$ GeV/$c^2$ (680 pb$^{-1}$) [6]. Understanding the energy scale of calorimeters for hadronic jets is a crucial component for this measurement. It has been achieved by reconstructing the $W$ boson mass using $W \to q\bar{q}$ candidates in the $t\bar{t}$ events themselves. This is shown in Figure 7.

Using also the measurements by the D0 experiment, we derive the combined top quark mass of $m_t = 171.4 \pm 1.2 \pm 1.8$ GeV/$c^2$. The precision has already surpassed the Run-II (2 fb$^{-1}$) goal of 3 GeV/$c^2$ .

As noted earlier, a new measurement of the $W$ boson mass has been performed by CDF recently. Combining it with top quark mass measurements provides indirect information on the Higgs boson. Figure 8 shows the new results, along with a constraint on the standard model Higgs boson mass, which is $80\,^{+36}_{-26}$ GeV/$c^2$, and less than 153 GeV/$c^2$ at 95% CL.

Other production and decay properties of the top quark will also be measured precisely, including $t\bar{t}$ spin correlations and $W^{\pm}$ boson helicity. Y. Takeuchi (Tsukuba) has been working on spin correlations using the dilepton channel, and N. Kimura (Tsukuba) attempts to measure initial parton fractions ($q\bar{q}$ vs. gluons) for $t\bar{t}$ production. Single top quark production should be observed as we accumulate more data, which should allow a direct measurement of the partial width $\Gamma(t \to W^+b)$ and a determination of CKM matrix element $|V_{tb}|$ to about 13%. Also, searches have been performed for new particles such as a charged Higgs boson through the top decay $t \to H^+b$, and for new resonant states decaying into $t\bar{t}$ pairs. J. Naganoma (Waseda) has been performing the latter analysis, in particular the searches for resonances predicted by the top-color model.

## 1.3 Bottom quark physics

One of the primary goals in $B$ physics at CDF was to observe $B_s^0$-$\bar{B}_s^0$ oscillations and measure their frequency $\Delta m_s$. The goal has now been achieved. CDF uses the silicon vertex trigger (SVT) to collect and reconstruct fully the hadronic decays of the $B_s^0$ meson, such as $\bar{B}_s^0 \to D_s^+\pi^-$. They allow a precise determination of the $B_s^0$ meson momentum on an event-by-event basis, leading to a superior proper time resolution. For a modest value of $\Delta m_s$, the partially reconstructed semileptonic decays $\bar{B}_s^0 \to \ell^-\bar{\nu}D_s^+X$ are also useful. Such signals have been observed and are shown in Figure 9. To look for possible $B_s^0$-$\bar{B}_s^0$ oscillations, an amplitude analysis has been employed. This is shown in Figure 10, where the amplitude of the oscillations is shown as a function of the assumed oscillation frequency $\Delta m_s$. The data indicate the oscillations at a frequency of about 17.7 ps$^{-1}$. The probability that background fluctuations produce such a spurious signal is estimated to be $8 \times 10^{-8}$, which corresponds to a Gaussian significance of more than $5\sigma$. Therefore, the $B_s^0$-$\bar{B}_s^0$ oscillations are established. The oscillatory behavior can be seen directly by examining the asymmetry between the unmixed and mixed decays as a function of the proper decay time (Figure 11 (left)). The oscillation frequency is determined from the likelihood distribution (Figure 11 (right)) to be [7]

$$\Delta m_s = 17.77 \pm 0.10 \pm 0.07 \text{ ps}^{-1}.$$

It provides a precise determination of the Cabibbo-Kobayashi-Maskawa matrix elements $|V_{td}/V_{ts}|$. Using lattice QCD calculations [8] of the $B$ meson decay constants and bag parameters, we extract [7]

$$\left|\frac{V_{td}}{V_{ts}}\right| = 0.2060 \pm 0.0007 \,{}^{+0.0081}_{-0.0060}.$$

The value is consistent with information obtained from other measurements, and represents a significant improvement in precision.

## 1.4 New particle searches

Searches for the Higgs boson, supersymmetric particles and other new particles have been performed. Cross sections for the standard model Higgs boson production at the Tevatron is shown in Figure 12 for various subprocesses. The largest contribution comes from the single production through gluon fusion, with the top quark in the loop. Associated production with weak bosons $W^{\pm}H$ and $Z^0H$ are smaller. The decay branching fractions of the Higgs boson are shown in Figure 13. At a low mass, below 120 GeV/$c^2$, the decay to $b\bar{b}$ pairs is dominant, while at high mass the decays to weak boson pairs become dominant.

CDF has searched for the Higgs boson production using many different final states. The first, aimed at a low mass Higgs, looks for the associated production $\bar{p}p \to VHX$, where $V$ is a weak gauge boson $W^{\pm}$ or $Z^0$, with the $W^{\pm}$ ($Z^0$) boson decaying into $\ell^{\pm}\nu$ ($\nu\bar{\nu}$) pairs, and the Higgs boson to $b\bar{b}$ pairs. The $b$ quark jets are identified with displaced vertices. The main background comes from heavy flavor production in association with the $W$ boson, and top quark pair production. The number of events as well as the di-jet mass distribution (Figure 14) are examined for possible production of the Higgs boson. No excess of events is found in 1 fb$^{-1}$ of data, and upper limits on the Higgs boson production cross section are set, in the range from 3.9 to 1.6 pb, depending on the assumed Higgs boson mass (110 to 150 GeV/$c^2$) [9]. They are roughly ten times larger than the standard model predictions. Y. Kusakabe and T. Masubuchi have performed the analysis.

The second analysis looks for single production of the Higgs boson followed by its decays to $W$ boson pairs. The channel is sensitive for high mass Higgs. The $W^+W^-$ final state is identified with their decays to leptons, thus two energetic leptons and large missing transverse energy and nothing else. The dominant background comes from electroweak $W^+W^-$ production, which leads to the same signature. However, there exists a difference in event topology, for example the lepton azimuthal angle correlations. Again, no excess of events is observed and upper limits on Higgs production have been placed.

The results from different analyses are combined and summarized in Figure 15, where the obtained upper limits on cross sections are normalized to standard model predictions. The limits are roughly ten times larger than the predictions. Various attempts at increasing the sensitivity are vigorously pursued.

Some extensions of the standard model predicts existence of leptoquarks, particles carrying both quark and lepton quantum numbers. A search is performed for pair production of the third generation vector leptoquarks, which decay to a tau lepton and a $b$ quark. One of the tau leptons is detected through the leptonic decay to an electron or a muon, and the other through hadronic decays. No excess of events above the expected backgrounds are found. A lower limit on the leptoquark mass of 317 (251) GeV/$c^2$ is placed assuming the Yang-Mills (Minimal) couplings [10], as illustrated in Figure 16. T. Akimono (Tsukuba) has performed the analysis.

# 2 Detector Operations and Upgrades

## 2.1 Detector operations

The original upgrades to the CDF detector for Run II have been completed for a few years now. The involvement and contributions of the Japan group included :

- plug calorimeter (Tsukuba)
- silicon detectors SVX-II (Hiroshima, Okayama) and ISL (Tsukuba, Osaka City)
- data acquisition system : consumer server/logger (Tsukuba, Nagasaki), silicon vertex trigger (Tsukuba), and online monitoring (Waseda, Tsukuba)
- muon detector system (Waseda)
- time-of-flight counters (Tsukuba)
- silicon detectors for Run-IIb (Tsukuba, Okayama)
- central calorimeter preshower detector (Tsukuba)

Now that the experiment is in a stable data-taking mode, the detector activities have mostly shifted to daily operations and monitoring.

However, there are still activities for further upgrades of the detector designed for expected increase in the Tevatron luminosity. We describe them here in the following subsections.

## 2.2 Consumer server/logger

M. Shimojima (Nagasaki), and T. Masubuchi and H. Miyake (Tsukuba) are currently responsible for the consumer-server/logger system, which, as part of the online data acquisition system, receives events from the level-3 trigger and sends to disk and tape storage devices as well as to online monitoring programs. In the original design of the system, the data transfer rate is 20 MB/s (or 80 events per second) and it has been achieved. However, with the continuous improvements in the accelerator luminosity, an upgrade was needed. The upgrade has been implemented in several stages, and from 2004 to 2005 a new software program was developed that allows recording of data in parallel. It has been operational already and has achieved a recording rate of 45 MB/s. In 2006 a new hardware system based on a PC farm was introduced. It has been operational since November 2006 and has achieved a rate of 60 MB/s. Beyond that, gradual improvements to the farm and software would bring us to close to 100 MB/s.

## 2.3 Silicon vertex trigger SVT

SVT is a hardware at the second level of the trigger system and utilizes information from the silicon vertex detector (SVX-II) and selects tracks that have large impact parameters with respect to the production point, which is approximated with the position of the Tevatron beam. The device is implemented in Run II for the first time and has been operational very successfully. It has enabled CDF to collect particles originating from decays of long-lived heavy quark hadrons such as $D$ and $B$ mesons, and to reconstruct their decays which include only hadrons in the final state, such as $\bar{B}_s^0 \to K^+K^-$ and $\bar{B} \to D\pi$.

The device also needed a speed-up for operations under high luminosity. From 2005 to 2006, both hardware and software were upgraded, and significant improvements in the processing time have been achieved. T. Maruyama and T. Kubo (Tsukuba) are involved in the SVT work.

# References


[1] "First Measurement of the $W$ Boson Mass with CDF in Run II", CDF Collaboration, CDF public note 8665 (2007).

[2] "Measurement of $W\gamma$ and $Z\gamma$ Production in $p\bar{p}$ Collisions at $\sqrt{s} = 1.96$ TeV", CDF Collaboration, CDF public note at http://fcdfwww.fnal.gov/physics/ewk/2006/wgzg/ (2006).

[3] "Top Pair Production Cross Section in Lepton + Jets Channel with Displaced Vertex", CDF Collaboration, CDF public note 8110 (2006).

[4] "A Measurement of the $t\bar{t}$ Production Cross Section Using Dileptons", CDF Collaboration, CDF public note 8103 (2006).

[5] "Measurement of the $t\bar{t}$ Production Cross Section in the All-hadronic Channel", CDF Collaboration, CDF public note 8402 (2006).

[6] "Measurement of the Top Quark Mass in the Lepton + Jets Channel Using the Template Method", CDF Collaboration, CDF public note 8402 (2006).

[7] "Observation of $B_s^0$-$\bar{B}_s^0$ Oscillations", A. Abulencia *et al.*, Phys. Rev. Lett. **97**, 242003 (2006).

[8] M. Okamoto, Proc. Sci. LAT2005, 103 (2005) [arXiv:hep-lat/0510113].

[9] "Search for Standard Model Higgs Boson Production in Association with $W$ Boson at CDF with 1 $\mathrm{fb}^{-1}$", CDF Collaboration, CDF public note 8390 (2006).
"Search for Higgs Boson Production in 1.96-TeV Proton-Antiproton Collisions", Yoshiaki Kusakabe, Ph. D. Thesis, Waseda University, December 2006.

[10] "Search for Third Generation Vector Leptoquarks in Run II", CDF Collaboration, CDF public note 8309 (2006).
"Search for Third Generation Vector Leptoquarks in 1.96-TeV Proton-Antiproton Collisions", Takashi Akimoto, Ph. D. Thesis, University of Tsukuba, February 2007.

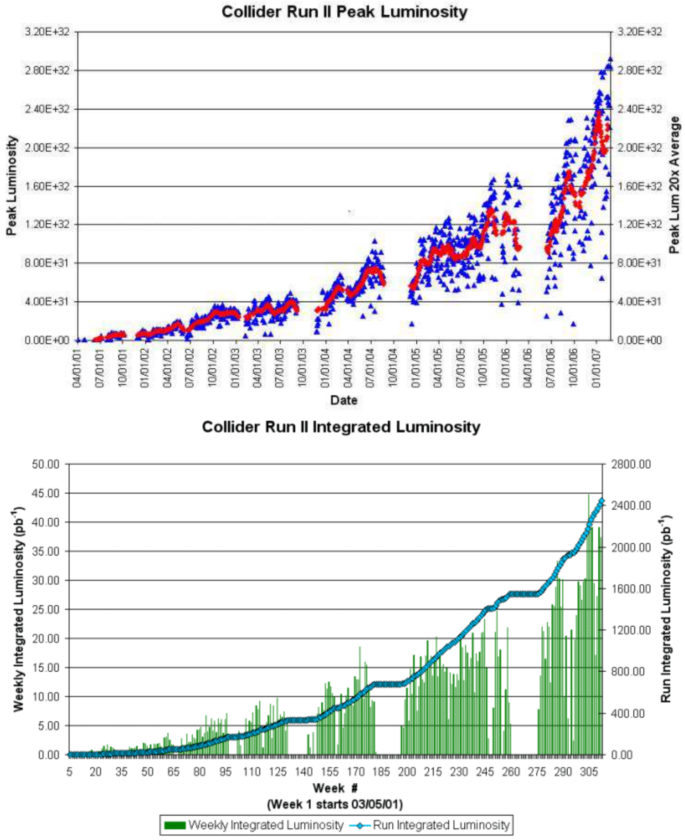


Figure 1: Tevatron performance in Run II. Top: instantaneous luminosity at the beginning of each store. Bottom: integrated luminosity delivered by week.

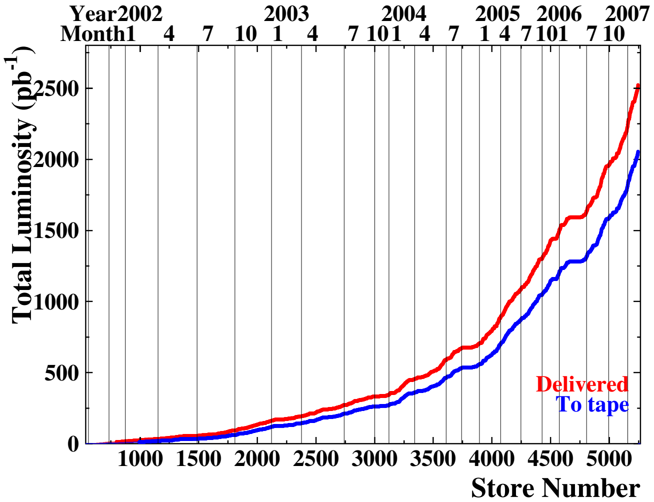


Figure 2: Integrated luminosity (top) delivered to and (bottom) recorded by CDF in Tevatron Run II.

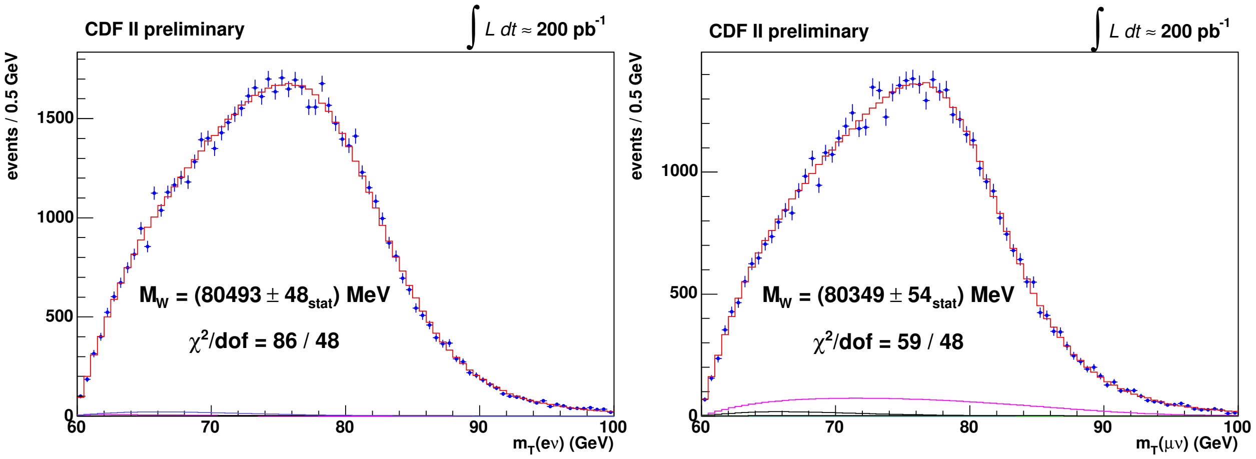


Figure 3: Transverse mass distribution of $W^\pm \to e^\pm\nu$ (left) and $\mu^\pm\nu$ (right) candidates and a measurement of the $W^\pm$ boson mass using 200 pb$^{-1}$ of Run-II data.

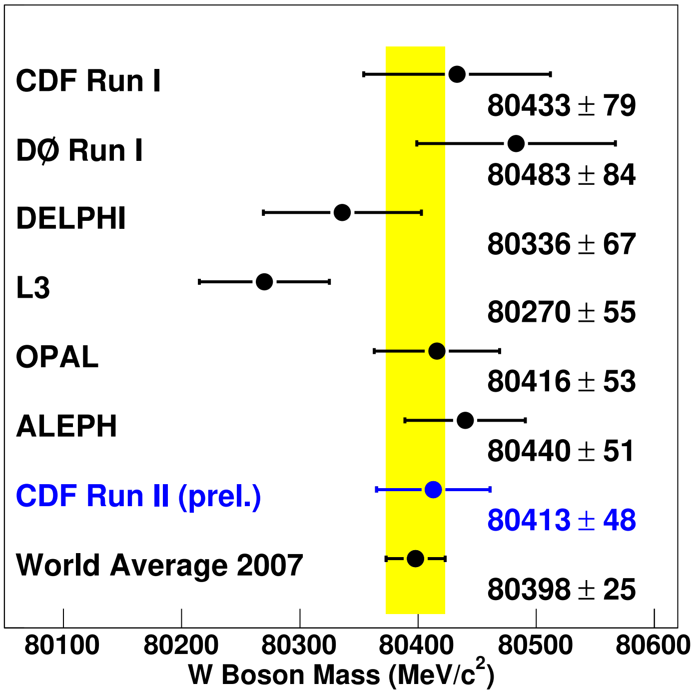


Figure 4: A summary of $W^\pm$ boson mass measurements.

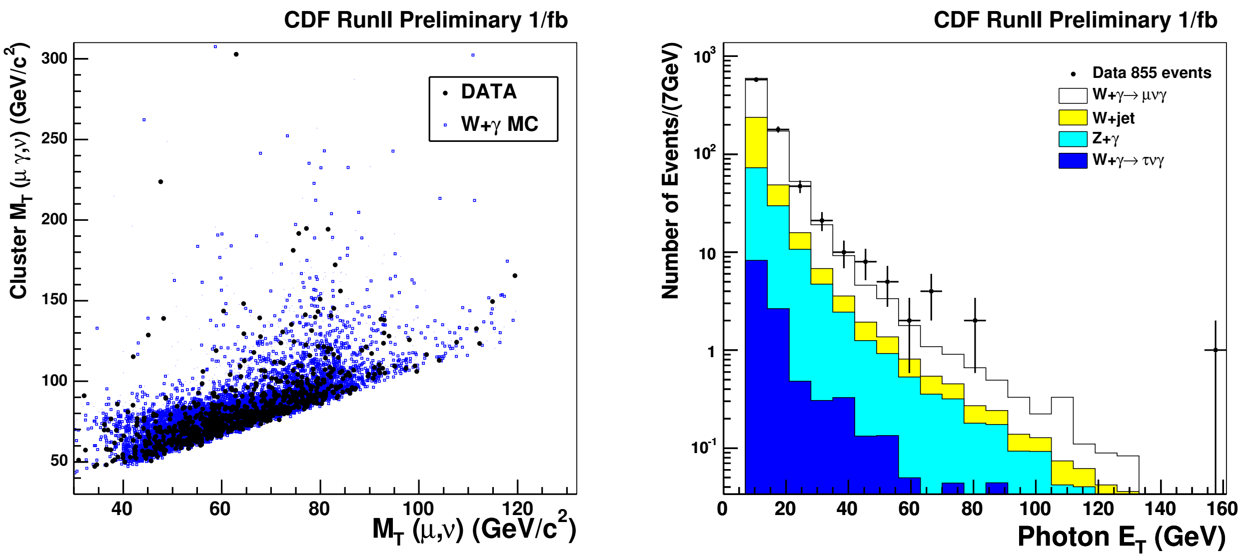


Figure 5: Transverse mass of the lepton-photon-neutrino system vs. lepton-neutrino system (left), and photon transverse momentum distribution (right), in $W\gamma$ pair production candidate events.

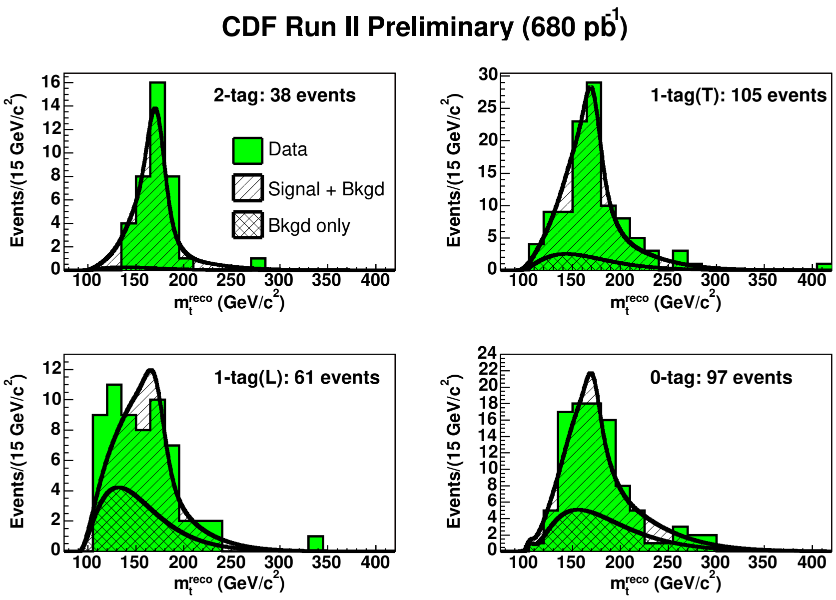


Figure 6: Top quark mass measurement from the lepton + jet channel in Run II data (680 pb$^{-1}$) with the template method. Reconstructed top quark mass distributions from subsamples corresponding to the number of tagged $b$-quark jets are shown.

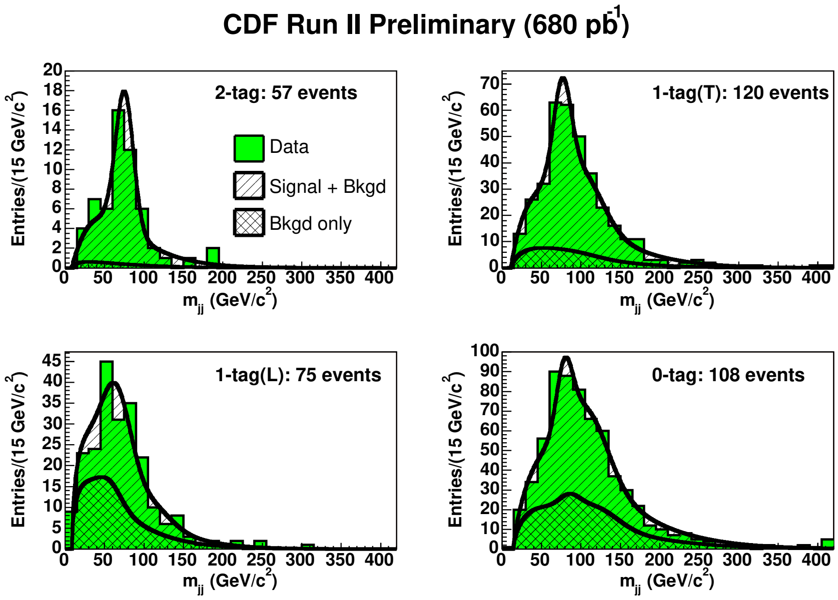


Figure 7: Top quark mass measurement from the lepton + jet channel in Run II data (680 pb$^{-1}$) with the template method. Di-jet mass distributions corresponding to the decay $W \to q\bar{q}'$ are shown.

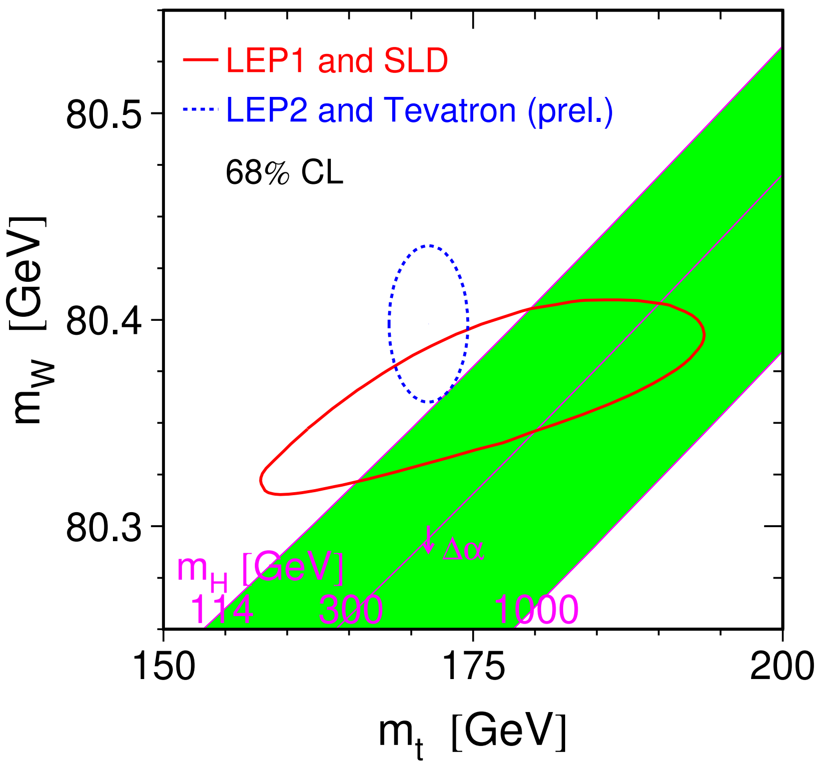


Figure 8: Measurements of the top quark and $W$ boson masses, and indirect information on the Higgs boson mass.

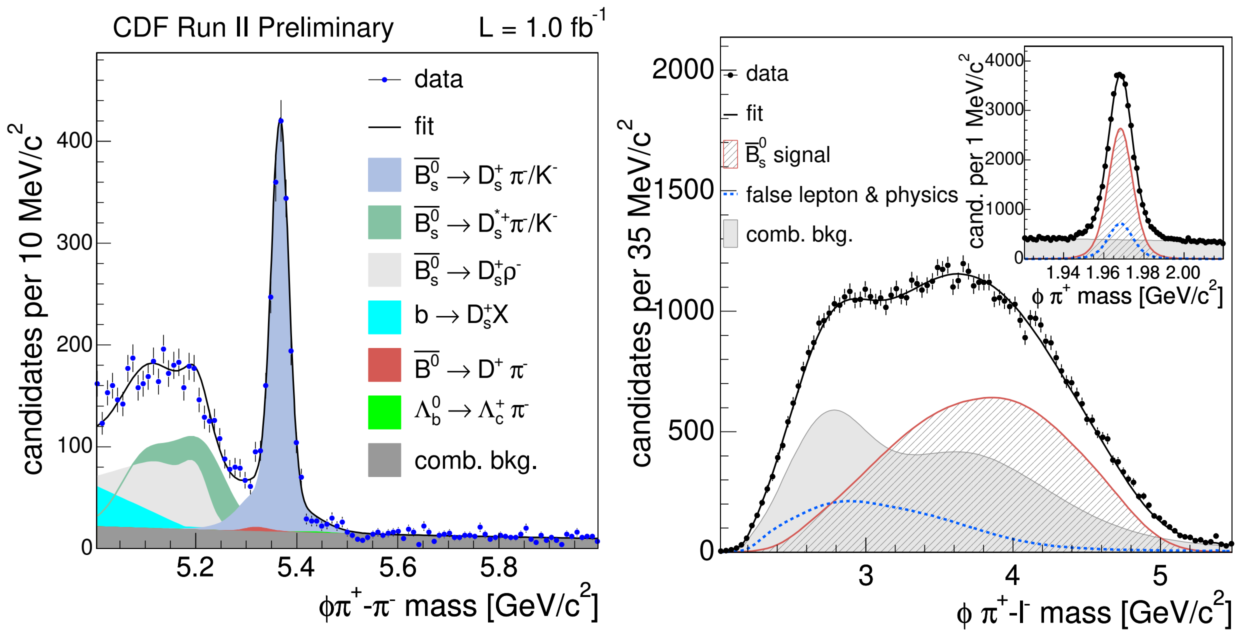


Figure 9: $B_s^0$ meson signals. Left: $\bar{B}_s^0 \to D_s^+\pi^-$, $D_s^+ \to \phi\pi^+$. Right: $\bar{B}_s^0 \to D_s^+\ell^-\bar{\nu}X$, $D_s^+ \to \phi\pi^+$.

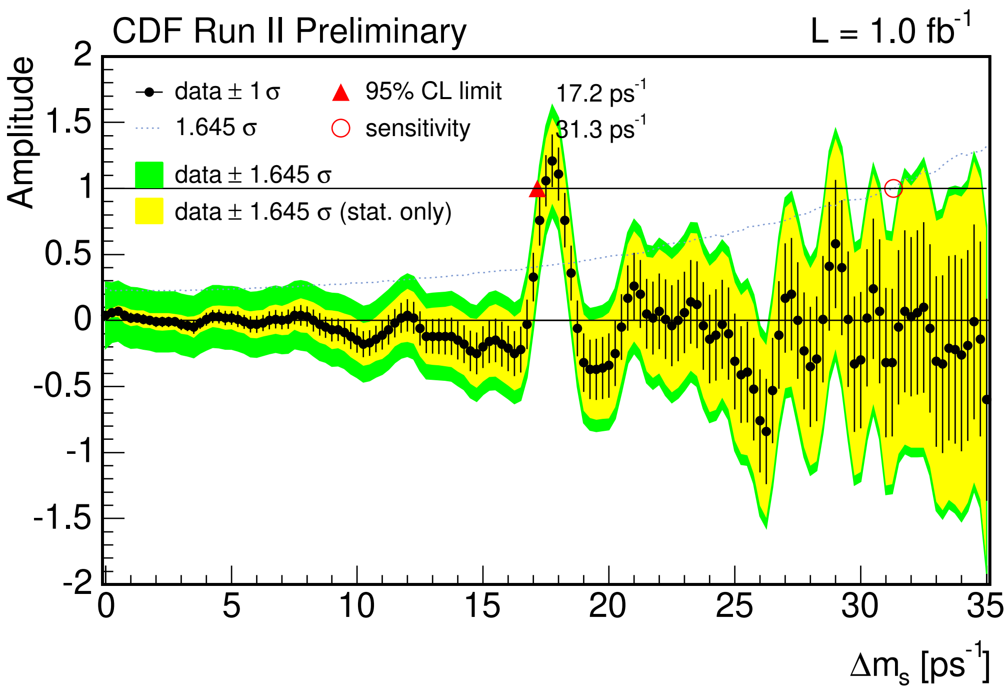


Figure 10: Search for the $B_s^0$-$\bar{B}_s^0$ oscillations. The amplitude of possible oscillations is shown as a function of the frequency $\Delta m$. The experimental data indicate oscillations with a frequency of about 17.7 ps$^{-1}$.

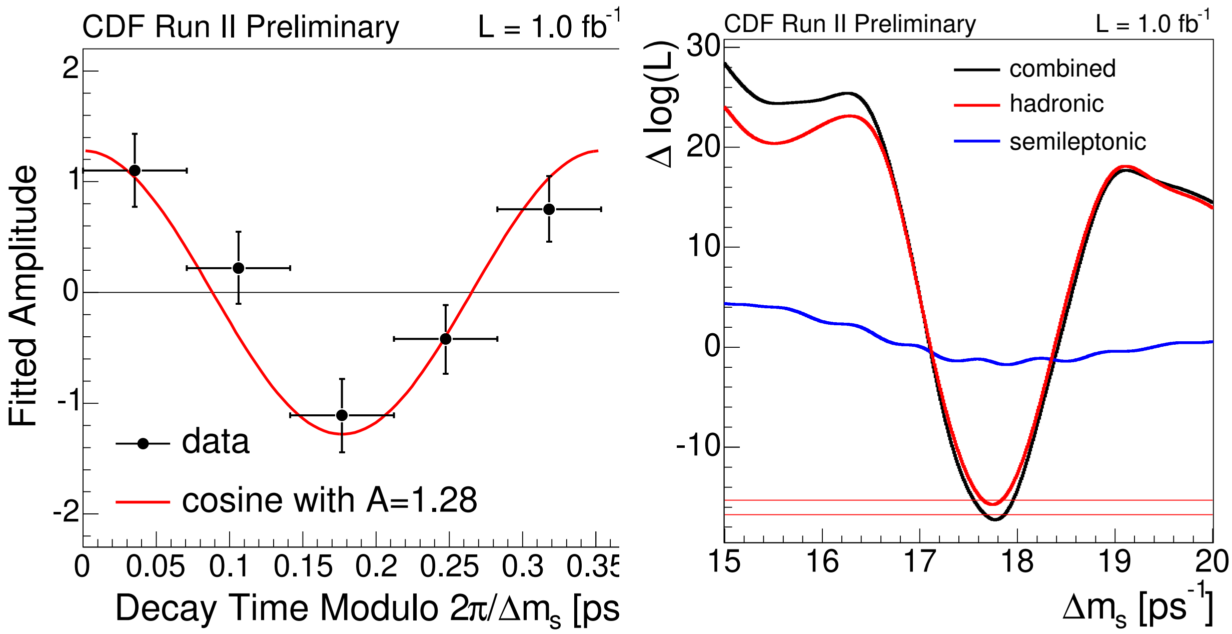


Figure 11: Left: $B_s^0$ vs. $\bar{B}_s^0$ asymmetry distribution as a function of the decay time, folded in to the measured oscillation period. Right: Likelihood distribution for $\Delta m_s$ measurement.

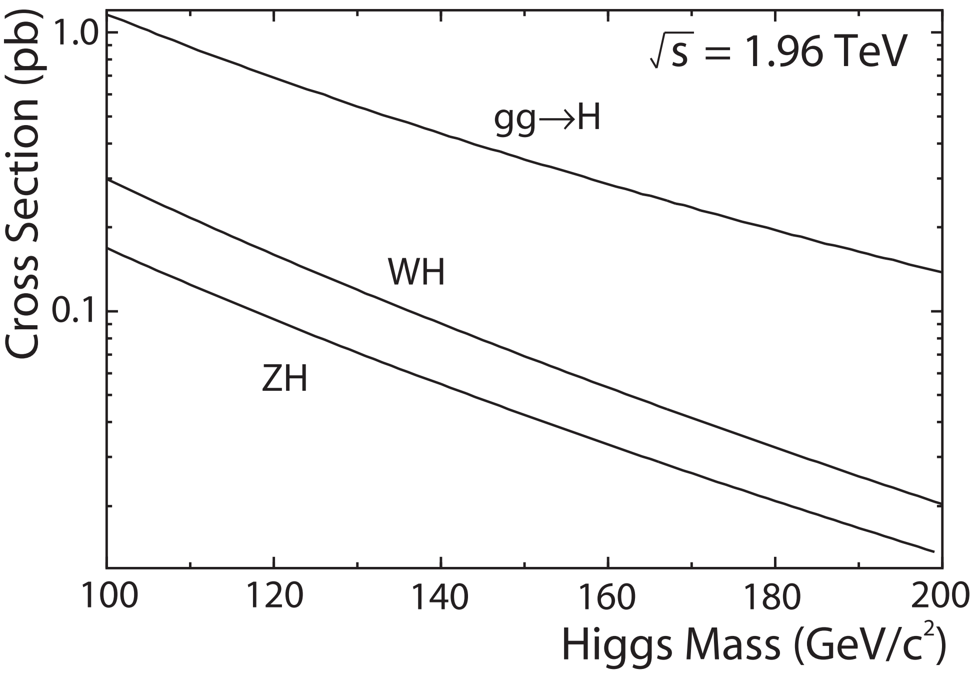


Figure 12: Top: Cross section for the production of the standard model Higgs boson at Tevatron. Bottom: Branching fractions of the standard model Higgs boson to various final states. Both plots show dependences on the Higgs boson mass.

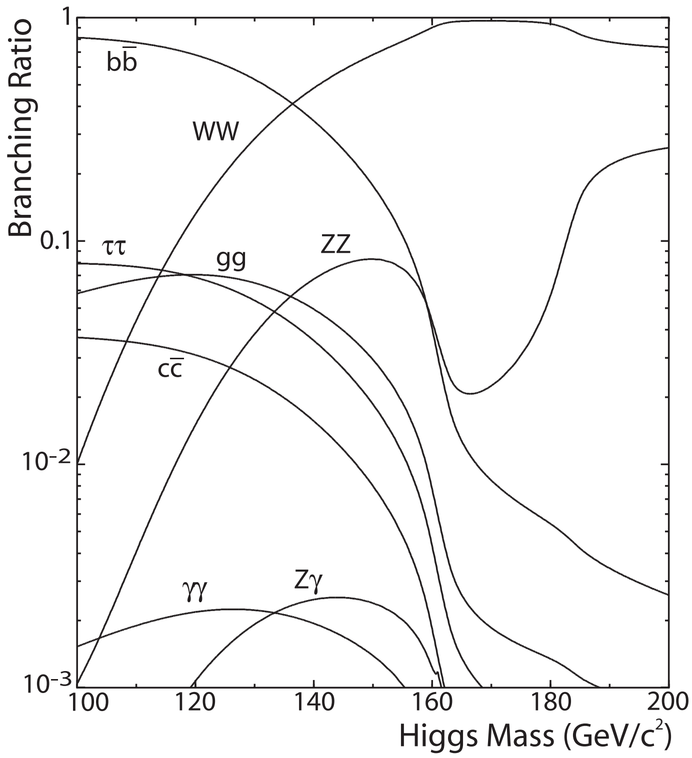


Figure 13: Branching fractions of the standard model Higgs boson to various final states. Both plots show dependences on the Higgs boson mass.

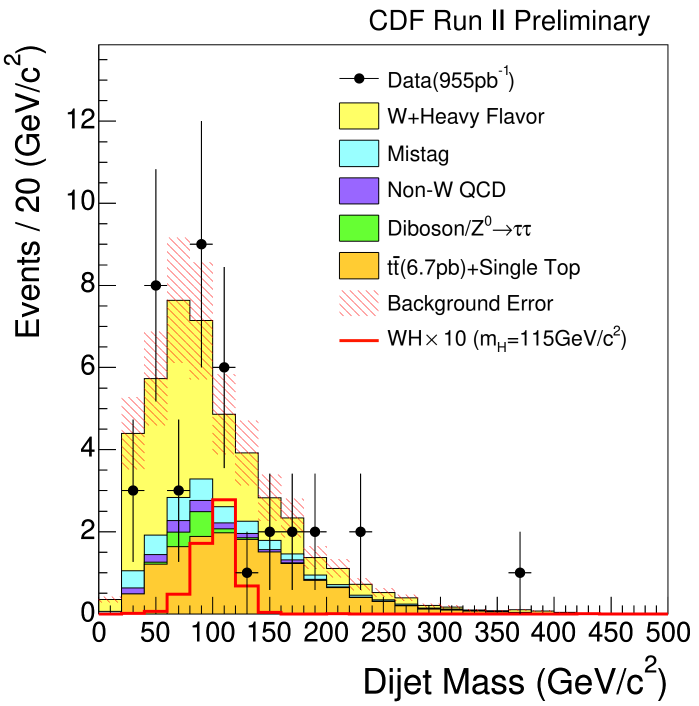


Figure 14: Higgs boson search in the $p\bar{p} \to W^{\pm}HX \to (\ell^{\pm}\nu)\,(b\bar{b})\,X$ channel. Invariant mass distribution of the two $b$-quark candidate jets produced in association with a $W$ boson.

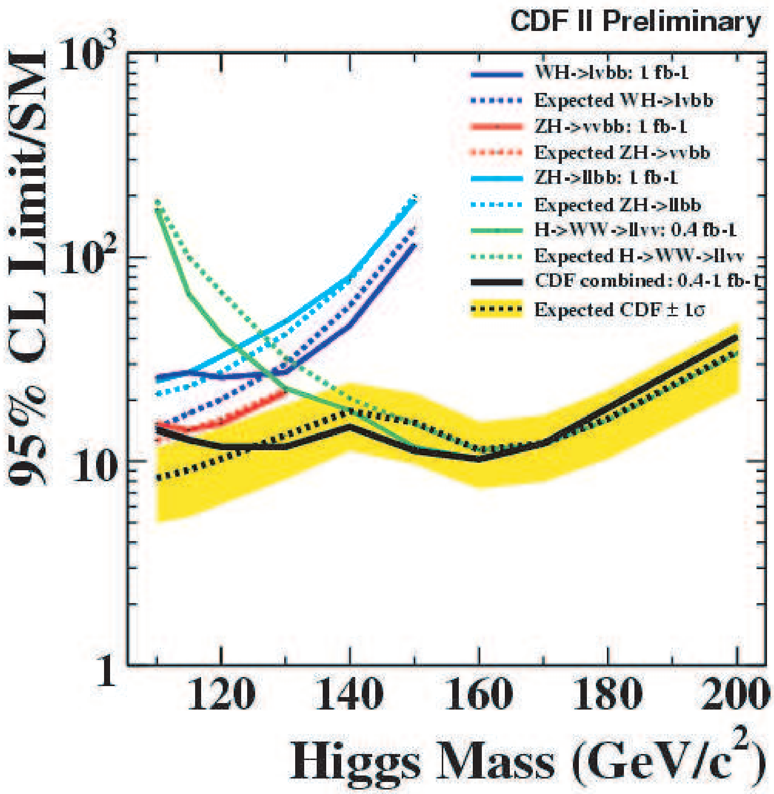


Figure 15: Summary of CDF results on the searches for the standard model Higgs boson. The experimental upper limits on production cross sections, normalized to the theoretical predictions, are shown for all search channels.

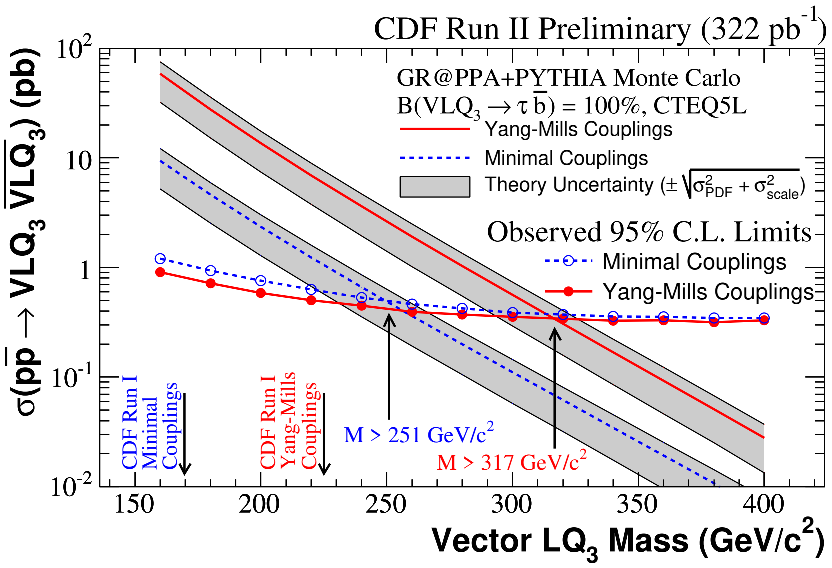


Figure 16: Search for production of the third generation leptoquarks using their decays to tau leptons and $b$ quarks.